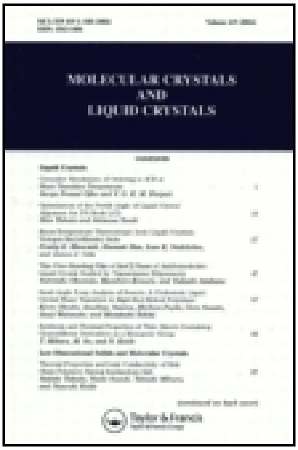

Molecular Crystals and Liquid Crystals
Publication details, including instructions for authors and subscription information:
http://www.tandfonline.com/loi/gmcl20

The characterization of carbon nitride alloy thin films deposited by pulsed laser deposition

M. Rusop [a], X. M. Tian [a], T. Soga [a], T. Jimbo [a] [b] & M. Umeno [c]

[a] Department of Environmental Technology and Urban Planning, Nagoya Institute of Technology, Nagoya, 466-8555, Japan

[b] Research Center for Micro Structure Devices, Nagoya Institute of Technology, Nagoya, 466-8555, Japan

[c] Department of Electronic Engineering, Chubu University, Kasugai, 487-8501, Japan

Version of record first published: 18 Oct 2010

To cite this article: M. Rusop, X. M. Tian, T. Soga, T. Jimbo & M. Umeno (2002): The characterization of carbon nitride alloy thin films deposited by pulsed laser deposition, Molecular Crystals and Liquid Crystals, 386:1, 89-96

To link to this article: http://dx.doi.org/10.1080/713738828

Mol. Cryst. Liq. Cryst., Vol. 386, pp. 89–96
Copyright © 2002 Taylor & Francis
1058-725X/02 $12.00 + .00
DOI: 10.1080/10587250290113240

THE CHARACTERIZATION OF CARBON NITRIDE ALLOY THIN FILMS DEPOSITED BY PULSED LASER DEPOSITION

M. Rusop, X. M. Tian, and T. Soga
Department of Environmental Technology and Urban Planning

T. Jimbo
Department of Environmental Technology and Urban Planning
Research Center for Micro Structure Devices, Nagoya Institute of Technology, Nagoya 466-8555, Japan

M. Umeno
Department of Electronic Engineering, Chubu University, Kasugai 487-8501, Japan

Carbon nitride (CN_x) alloy thin films were deposited by pulsed laser deposition (PLD) with varying nitrogen gas pressure (NP) from 0.1 to 800 mTorr at 20°C of substrate temperature (ST) and with varying ST from 20 to 500°C at 0.8 Torr of NP. The effects of the NP and ST on the composition, structural and electrical properties of the nitrogen (N) incorporated camphoric carbon (CC) films have been investigated by standard measurement techniques. We found that, the amorphous structure of CN_x films can be changed by NP and ST, and the CN_x films with high N content have relatively high electrical resistivity.

Keywords: nitrogen; carbon nitride; carbon nitride alloy; amorphous carbon nitride; amorphous carbon; pulsed laser deposition

INTRODUCTION

Pulsed laser deposition (PLD) technique used for film preparation has become popular for its simplicity, versatility and capability to generate highly energetic carbon (C) species large tetrahedral (sp^3) fractions which enhances the synthesis of high quality films with good mechanical and optical properties [1]. The properties of crystalline phase of C nitride (CN_x) alloy thin films was reported by Liu and Cohen [2,3]. They have proposed β-CN_x, a form of CN_x alloy analogous to β-Si_3N_4, should have hardness closer to diamond, a super hard material. CN_x films already have shown considerable interest in the field of protective coating for magnetic and optical material [4]. It has been reported that, photoconductivity from amorphous-CN_x (a-CN_x) films is encouraging for its application in optoelectronic devices in future [5]. However, undoped C is slightly p-type and doping is essential for the application of C in electronic devices. The objective of this work is to investigate the effect of nitrogen (N) gas into amorphous carbon (a-C) films by ablating C from a camphoric carbon (CC) soot target in N ambient using PLD. The motivation behind this attempt is synthesis of CN_x films and doping of C in order to convert undoped p-type C to n-type.

EXPERIMENTAL

We report the effects of N gas pressure (NP) range from 0.1 to 800 mTorr at 20°C of substrate temperature (ST) and ST range from 20 to 500°C at 800 mTorr of NP, on the deposition of CN_x films and compared with sample A, which was deposited at 800 mTorr of NP and 20°C of ST. To investigate the effects of NP, the CC target was ablated by XeCl excimer PLD, which operates at a wavelength of 308 nm for 900 laser shots. At a repetition rate of 2 Hz and 20 ns pulse width was focused at a 45° angle onto a target by a ultraviolet grade plano-convex lens. The laser fluence was maintained range from 1.8 to 2.2 J/cm^2 by adjusting the laser energy and the lens to target distance for adjusting the laser spot size. The substrate was mounted on a metal substrate stage holder parallel to the CC target at a distance of 45 mm. In order to ensure a uniform ablation rate, the CC target was rotate at each 50 shots. The deposition chamber was evacuated to a base pressure approximately at 2×10^{-5} Torr using a turbomolecular pump. After that N gas ambient was allowed until the chamber pressure is at setting NP in range from 0.1 to 800 mTorr. To investigate the effects of ST, the CC target was ablated using the above procedure and ST was set in range from 20 to 500°C at 800 mTorr of NP. The reference sample of a-C film, thereafter referred to as sample A, has also been prepared using the above procedure at 20°C of ST and 800 mTorr of NP. The composition, structural, optical and electrical properties of the films have been investigated using Auger Electron Spectroscopy (AES), Fourier Transform Infrared Spectroscopy (FTIR), X-ray Photoelectron Spectroscopy (XPS), UV-Visible Spectroscopy and Four probe resistance measurement.

RESULTS AND DISCUSSIONS

Compositional chemical analyses of the deposited films were performed by AES. Figure 1 illustrates the AES spectra of sample A and a-CN_x films, showing that the films were mainly composed of C and N. The existence of a small oxygen signal was a result of air exposure during sample transport. The spectra are compared, revealing that the peak is increases with the increases of NP (Fig. 1a) and ST (Fig. 1b). The intensity of N peak in the low energy region corresponds to the NP and ST, indicating that N was effectively doped into the a-C films during deposition and also implying that N content in the films increases with the increases of NP and ST at fixed ST and NP respectively as the peak intensity shows the increasing tendency.

FTIR transmittance spectra were measured in the wave number in range 600–2500 cm^{-1} (Fig. 2) show for a-CN_x films, contributions around 1350 and 1550 cm^{-1} were initiated from disordered (D band) and graphite like (G band) CN bonds [6]. Another contribution, at around 1212–1265 cm^{-1}, was due to symmetric tetrahedral CN bond [7]. Figure 2a shows FTIR spectra of sample A and a-CN_x films with various NP at fixed ST. At 0.1 mTorr single broad band centered at around 1365 cm^{-1}, almost unchanged up to 1 mTorr, but rapidly shifted later at 10 mTorr into a single broad band centered at around 1550 cm^{-1}. The FTIR absorption almost unchanged with higher NP up to 30 mTorr and gradually resolved into two

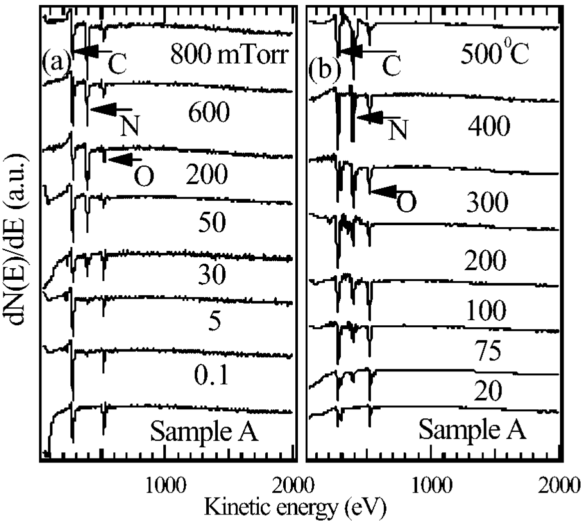

FIGURE 1 The Auger electron spectra of sample A and a-CN_x films with various: a) nitrogen gas pressures, and b) substrate temperatures.

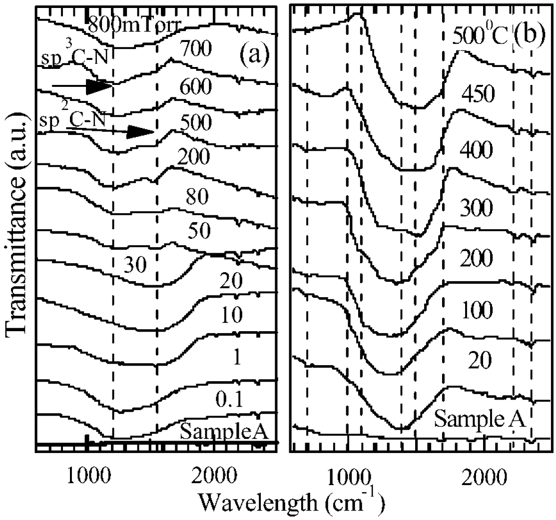

FIGURE 2 The FTIR spectra obtained from sample A and a-CN$_x$ films with various: a) nitrogen gas pressures, and b) substrate temperatures.

smaller bands located at 1550 and 1200 cm^{-1}. With higher NP, these two bands become more prominent but transformed later at 600 mTorr, into a single broad band centered at around 1200 cm^{-1}, and almost unchanged with higher NP thereafter. Above 30 mTorr, the G band seems to be suppressed gradually, together with the enhancement of the sp^3 C-N bonds. This indicates no modification of the binding geometry at low NP up to 1 mTorr and a modification of the binding geometry with the transformation of the sp^3 C-N bonds into sp^2 C-N binding state as NP increased up to 10 mTorr and almost in stable condition with the addition of NP up to 30 mTorr. Whereas, a modification of the binding geometry with the transformation of the sp^2 C-N bonds into sp^3 C-N binding state as NP increased up to 600 mTorr and almost in stable condition with the addition of NP up to 800 mTorr. Figure 2b shows FTIR spectra of sample A and a-CN$_x$ films with various ST at fixed NP. Band 1 at around 700 cm^{-1} is due to the out-of-plane bending mode for the graphite-like domain [8]. Broad absorption band 2 at 1000–1700 cm^{-1} indicates that the film structure is predominantly amorphous with sp^2 C vibration modes, and is related to Raman active D and G modes [9]. Band 3 at 1100–1400 cm^{-1} and band 4 at 1500–1700 cm^{-1} and band 5 at around 2200 cm^{-1} are due to C-N, C=C and/or C≡N stretching vibration modes, respectively [10]. In our spectra, bands 3, 4 and 5 are very weak and as ST is increased, starting from around 200°C the broad absorption band 2 becomes narrow and although small, the intensity of band 3, 4 and 5 increase gradually up to 400°C and decrease thereafter. This indicate the components of the C-N, C=N, C = C and C ≡ N bonds increases with the ST up to 400°C and decrease thereafter, which is also confirmed by the XPS analyses. The broad band between 1000 and 1700 cm and the band centered at 2200 cm^{-1} do not appear in sample A. The absorption peak at around 2350 cm^{-1}, which is observed in a-CN_x and sample A film, can be attributed to the CO_2 stretching mode arising from oxygen contamination at the film surface [11].

The bonding state and chemical composition in the a-CN_x films were analyzed using XPS after the 0.5 keV Ar^+ ion etching of film surface for 3 min. C 1s peak position of sample A film is found to be at 284.8 eV, which is 1.0 eV lower than that of diamond at 285.8 eV. XPS shows the C 1s peak position is increased to 284.9 eV at 0.1 mTorr, may be due to the formation of C-N bond which caused the sp^3 bond increased. At fixed ST, the C 1s and N 1s peaks almost unchanged up to 1 mTorr. Further increase of NP, the C 1s and N 1s peaks become narrow, indicating the enhancement degree of crystallization in the films. Further, the C 1s peak shifts toward lower binding energy and approaches the binding energy of graphite at 284.25 eV at 30 mTorr. This indicates the bonding state of the films changes from low diamond-like sp^3 bonding to graphite like trihedral (sp^2) bonding. Above 30 mTorr, the C 1s peak shifts toward higher binding energy and reached at 284.6 eV at 800 mTorr. This indicates the bonding state of the films changes from graphite-like sp^2 bonding to diamond-like sp^3 bonding. The N/C ratio in the film is found to increase rapidly from 0.4% at 0.1 mTorr to 2.2% at 10 mTorr, after which it increases gradually up to 3.58% at 80 mTorr and saturates thereupon up to 3.69% at 800 mTorr. At fixed NP, C 1s peak position is decreased to 284.4 eV at 20°C may be due to the formation of C-N bond. With the increase in ST, the C 1s peak (Fig. 3a) becomes narrow and the N 1s peak (Fig. 3b) splits into two subpeaks indicating the enhancement degree of crystallization in the films. Further, as ST increases, the C 1s peak shifts toward lower binding energy and approaches the binding energy of graphite at 284.25 eV [12] when ST reaches 400°C. This shift can be explained as the bonding state of the films changes from low diamond-like sp^3 bonding to graphite-like sp^2 bonding with the increase in ST. On the other hand, the N 1s peak spectra showed asymmetric bands centered at around 400 eV. With the increases of the ST to 200°C, the N 1s spectrum splits into two bands located at around 400 and 398 eV. It implies a change in bonding structure. The N signal of the film deposited at 400°C can be deconvoluted (not shown) into two peaks at 398.4 and 400.5 eV. The chemical shift of 2.1 eV between these two components reflects two different binding states of N, which can be attributed to N≡C and N=C [13]. Thus, the observed chemical shift indicates that N atoms are bound to the

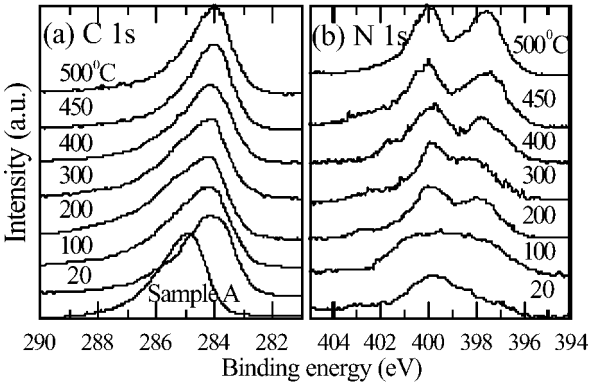

FIGURE 3 Effect of the substrate temperature on: a) the C 1s, and b) the N 1s core level spectra.

C atoms. The N/C ratio in the film is found to increase gradually from 3.69 to 15.05%, with an increase in the ST up to 400°C, hereafter it decrease at higher ST. With the increase in ST, the surface migration of C and N species will be enhanced, which will accelerate the chemical reaction between C and N and consequently improve the N content. However, at ST of higher than 400°C, N content in the film decreases because the stable C-N bonding only remains since the volatile bonding decomposes and N molecules released from the films.

The optical properties of the films are investigated by UV-Visible Spectroscopy measurements in the range of 200 to 2500 nm. The optical gap (E_g) and electrical resistivity (ρ) of sample A is 0.95 eV and 5.1×10^5 [Ω-cm], respectively. Figure 4a shows at fixed ST, the E_g of a-CN_x films is almost unchanged up to 1 mTorr compared with sample A and decreases thereafter to 0.83 eV at 10 mTorr after it decreases rapidly to 0.7 eV at 30 mTorr. With higher NP, it increases to 0.91 eV at 500 mTorr and almost constant thereafter to 0.93 eV at 800 mTorr. While, the ρ of a-CN_x films is increase initially to 5.5×10^6 [Ω-cm] at 0.1 mTorr, decreases with higher NP up to 1.8×10^2 [Ω-cm] at 30 mTorr. Above 30 mTorr, it increases rapidly to 5.5×10^6 [Ω-cm] at 500 mTorr and continuously increases thereafter up to maximum value of 8.7×10^6 [Ω-cm] at 800 mTorr. The increase in ρ with N incorporation, initially at 0.1 mTorr may be due to the reason that as N content increase from null, the incorporated N atoms compensated the dangling bands in the a-C structure and increase the sp^3 fraction. At low NP up to 1 mTorr and upon increasing of NP above 30 mTorr, the variation of E_g and electrical properties can be related to interstitial doping of N in C films through modifications of C-N bonding configurations by rearranging N of atoms. The increase in ρ with N incorporation may also due to the lattice vibrations

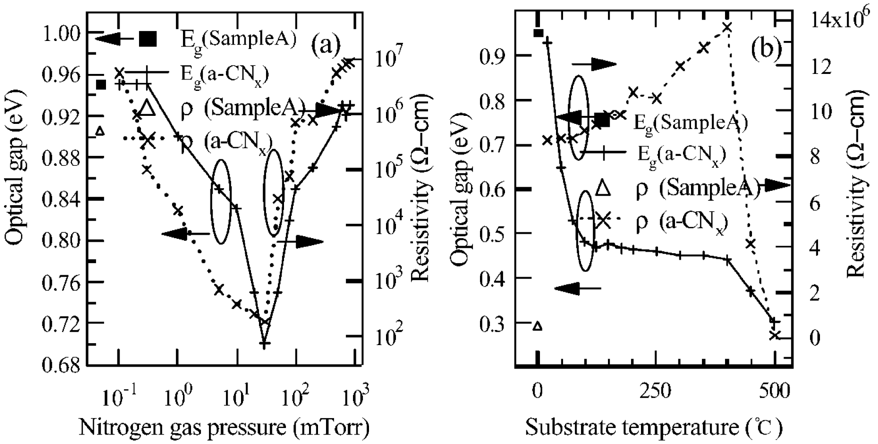

FIGURE 4 Dependance of optical gap and resistivity of sample A and a-CN$_x$ films on: (a) nitrogen gas pressure, and (b) substrate temperature.

leading to the scattering of the charge carriers by the N atoms and more amorphous nature of the C films. However from 1 to 30 mTorr, the variation of E$_g$ and electrical properties can be related due to carbonization of a-CN$_x$ films. Perhaps the doping of N accompanied by increase of NP up to 30 mTorr, increases crystallinity and substitutional doping of N thereby sharply decreases ρ. Figure 4b shows at fixed NP, the E$_g$ of a-CN$_x$ film decreases to 0.65 eV and the ρ is increases to 8.7×10^6 [Ω-cm] at 20°C compared with sample A. As ST increases, the E$_g$ decreases only a little, while ρ increases up to 1.36×10^7 [Ω-cm] at 400°C, making these a-CN$_x$ films interesting. The increases in ρ with N incorporation may be due to the lattice vibrations leading to the scattering of the charge carriers by the N atoms and more amorphous nature of the C films in the range between of 20 to 400°C. Variation of the optical and electrical properties can be related to interstitial doping of N in C films through modifications of C-N bonding configurations by rearranging N of atoms upon substrate heating. However above 400°C, both E$_g$ and ρ are drastically decreases up to 0.3 eV and 8.45×10^4 [Ω-cm] at 500°C, respectively. This is probably due to progress of the carbonization of the CN$_x$ films. Perhaps the doping of N accompanied by increase of ST above 400°C increases crystallinity and substitutional doping of N thereby sharply decreases ρ.

CONCLUSIONS

We have successfully deposited a-CN$_x$ films using CC soot target by PLD. The dependence of the ST and N gas ambient on the composition, structure, optical and electrical properties of the films was investigated. It is found that the amorphous structure of CN_x films can be changed by ST and the CN_x films with high N content have relatively high ρ. The variation of E_g and ρ show successful doping for the film deposited at low NP. The reduction in E_g and ρ, with increase of N content in the film is due to progress of the carbonization of C films. While, the increase in E_g and ρ with further increase of N content in C films are attributed to the structural modifications through the formation of some form of CN_x alloy.

REFERENCES

[1] Martin, J. A., Vazques, L., Bernard, P. *et al.* (1990). ***Appl. Phys. Lett.***, ***57***, 1742.
[2] Liu, A. Y. & Cohen, M. L. (1989). ***Science***, ***245***, 841.
[3] Liu, A. Y. & Cohen. (1990). ***Phys. Rev.***, ***B41***, 10727.
[4] Prioli, R., Zanette, S. I., Caride, A. O. *et al.* (1999). ***Diamond Relat. Mater.***, ***8***, 993.
[5] Nitta, S., Takada, N., Sugiyama, K. *et al.* (1998). ***J. Non-Cryst. Solids***, ***655***, 230.
[6] Hammer, P., Baker, M. A., Lenardi, C., & Gissler, W. (1997). ***J. Vac. Sci. Technol.***, ***A15***, 107.
[7] Wixom, M. R. (1990). ***J. Am. Ceram. Soc.***, ***73***, 1973.
[8] Nakayama, N., Tsuchiya, Y., Tamada, S. *et al.* (1993). ***Jpn. J. Appl. Phys.***, ***32***, 1465.
[9] Zeng, W. T., Broitman, E., Hellgren, N. *et al.* (1997). ***Thin Solid Films***, ***308***, 223.
[10] Aoi, Y., Ono, K., & Kamijo, E. (1999). ***J. Appl. Phys.***, ***86***, 2318.
[11] Bousetta, A., Lu, M., Bensaola, A., & Schults, A. (1994). ***Appl. Phys. Lett.***, ***65***, 696.
[12] Han, H. X. & Feldman, B. J. (1998). ***Solid State Comm.***, ***65***, 921.
[13] Rossi, F., Andre, B., Veen, A., Mijnarends, P. E. *et al.* (1994). ***Thin Solid Films***, ***253***, 85.